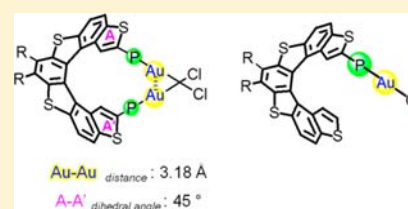


Gold(I) Complexes of Tetrathiaheterohelicene Phosphanes

Silvia Cauteruccio,[†] Annette Loos,[§] Alberto Bossi,[‡] Maria Camila Blanco Jaimes,[§] Davide Dova,[†] Frank Rominger,[§] Stefan Prager,^{||} Andreas Dreuw,^{||} Emanuela Licandro,^{*,†} and A. Stephen K. Hashmi^{*,§}[†]Dipartimento di Chimica, Università degli Studi di Milano, via Golgi 19, I-20133 Milan, Italy[§]Organisch-Chemisches Institut, Universität Heidelberg, Im Neuenheimer Feld 270, 69120 Heidelberg, Germany[‡]Istituto di Scienze e Tecnologie Molecolari, CNR, via Fantoli 16/15, I-20138 Milan, Italy^{||}Interdisziplinäres Zentrum für Wissenschaftliches Rechnen, Universität Heidelberg, Im Neuenheimer Feld 368, 69120 Heidelberg, Germany

ABSTRACT: New tetrathia[7]helicene-based (7-TH-based) gold(I) complexes **6** and **7** have been readily prepared by reaction of the respective phosphine ligands **2** and **3** with Au(tht)Cl in a 1:1 and 1:2 molar ratio, respectively. These complexes have been fully characterized by analytical and spectroscopic techniques as well as quantum chemical calculations. The molecular structure of dinuclear complex **7** has been determined by single-crystal X-ray diffraction, showing a gold–gold interaction of 3.1825(3) Å and a significant contraction of the 7-TH total dihedral angle. Au(I) complex **7** displays luminescence emission at room and low temperature in diluted solution and in the solid state. Quantum chemical calculations show that the luminescence emission at room temperature is primarily due to slightly perturbed fluorescence emission from purely $\pi\pi^*$ excited states of the conjugated helicene scaffold. At 77 K phosphorescence emission is displayed as well. Preliminary studies on the use of **6** and **7** as catalysts in typical Au(I)-catalyzed cycloisomerizations have demonstrated the reactivity of these systems in the intramolecular allene hydroarylations and the hydroxycarboxylation of allene-carboxylates.



INTRODUCTION

Gold chemistry is currently one of the most rapidly growing fields of chemistry because of its relevance to a large number of topics, including catalysis,¹ materials science,² and medicine.³ In particular, gold(I) complexes incorporating phosphines have been widely developed during the past few years, especially for their use as efficient and selective homogeneous catalysts in organic transformations,⁴ but also for their intriguing physical properties, including luminescence,⁵ as well as for their promising anticancer activity.⁶

Homogeneous catalysis promoted by Au(I) complexes has emerged as a powerful synthetic tool for organic synthesis,⁴ with phosphines and *N*-heterocyclic carbenes⁷ as the ligands of choice for gold(I)-based catalysts. Moreover, asymmetric gold-catalyzed reactions have been applied to a variety of transformations that provide versatile routes leading to the enantioselective formation of new carbon–carbon or carbon–heteroatom bonds.^{7a,8} On the other hand, several mono- and polynuclear organophosphane–Au(I) complexes have been spectroscopically investigated and reviewed in the literature due to their fascinating luminescence properties.⁵ So far, different types of electronic transitions have been indicated as the origin of their luminescence. Several parameters may influence the photophysical behavior of Au(I) systems, but the nature of the phosphine ligand often plays the key role.^{5,9}

Despite a large number of gold(I) complexes bearing different mono- or diphosphine ligands being studied, to the best of our knowledge no example of gold(I) complexes containing helical-based phosphines has been reported to date.

Helicenes are an extremely attractive class of conjugated molecules, which combine the electronic properties afforded by their conjugated system with the chiroptical properties provided by their peculiar helix-like structure, resulting from the ortho annulation of a series of aromatic and/or heteroaromatic rings.¹⁰

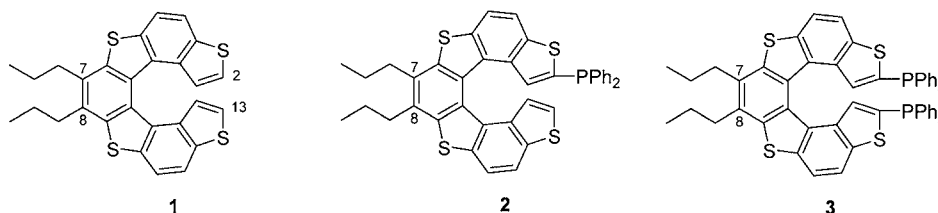
These structures display unique physicochemical properties, which have stimulated countless studies oriented toward chiroptical devices,¹¹ material chemistry,¹² organometallic species,¹³ and organocatalysis.¹⁴ In the general context of the growing interest in helical derivatives, we have focused our attention on the study of tetrathiahelicene (7-TH) derivatives, such as compound **1** (Chart 1), that represent a class of configurationally stable heterohelicenes with intrinsic asymmetry, potentially very interesting for applications in optoelectronics^{15–17} as well as new chiral ligands for both organic¹⁸ and organometallic catalysis.¹⁹ In addition, these systems can be easily and selectively functionalized at the α positions of the two terminal thiophene rings,²⁰ allowing the modulation of the chemical and physical properties by varying the nature of the substituents.

In the course of our studies on the applications of 7-TH derivatives in the field of the organometallic chemistry, we have described the synthesis of organometallic derivatives of tetrathia[7]helicenes for some ruthenium(II) and iron(II) complexes, which have been shown to be potential interesting

Received: March 5, 2013

Published: July 1, 2013

Chart 1. Structures of 7-TH 1 and Its Phosphane Derivatives 2 and 3

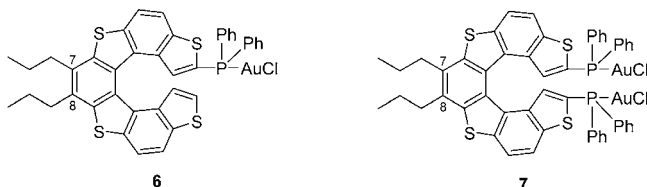


candidates for electro-optical and nonlinear optical (NLO) purposes.^{17a}

More recently, we have reported the synthesis of 7-TH-based phosphane derivatives like mono- and diphosphane 2 and 3 (Chart 1), which were isolated as air-stable borane adducts 4 and 5, respectively.¹⁹ In fact, alkyl chains in the 7- and 8-positions of the helical system improve the solubility of helicenes in organic solvents, but also render the phosphorus atoms more electron-rich and then more prone to air oxidation. The enantiopure *P*-(3) was employed by some of us as chiral ligand to form a chelated Rh complex, which was used in the asymmetric hydrogenation of the dehydroalanine achieving almost quantitative yield but a modest 40% ee.¹⁹

In view of our interest to further investigate the coordinating ability of phosphanes 2 and 3 toward transition metals, we decided to study innovative complexes of gold(I) with helical phosphines, especially with tetrathiahelicene-based phosphines as ancillary ligands. In this Article, we describe the synthesis and the characterization of gold(I) complexes 6 and 7 (Chart 2)

Chart 2. Structure of the Au(I) Complexes 6 and 7 under Investigation



prepared from phosphanes 2 and 3, respectively, along with the X-ray characterization of the dinuclear complex 7. In addition, a preliminary investigation of the luminescence properties of the dinuclear gold(I) complex 7 has been undertaken, and the emission data are reported. High-level quantum chemical calculations demonstrate the emission occurs from purely $\pi\pi^*$ excited states of the helical ligand scaffold. Finally, we also report a first study demonstrating the use of complexes 6 and 7 as catalysts in a set of typical Au(I) catalyzed cycloisomerization reactions.

EXPERIMENTAL SECTION

General. The syntheses of gold(I) complexes 6 and 7 were performed under an atmosphere of argon by means of standard Schlenk and vacuum-line techniques in flame-dried glassware. To monitor the progress of these reactions, thin-layer chromatography (TLC) was performed with Merck silica gel 60 F254 precoated plates. Anhydrous THF and CH_2Cl_2 (Aldrich) were purchased and purged with argon prior to use. Reagents obtained from commercial sources were used without further purification. Diborane adduct 5 was prepared as previously reported.¹⁹ $\text{Au}(\text{tht})\text{Cl}^{21}$ was prepared according to literature procedure. Melting points were determined with a Büchi 510 apparatus and are uncorrected. The ^1H , $^{13}\text{C}\{^1\text{H}\}$ spectra were recorded on the Bruker Avance 600 MHz Ultra Shield Plus

spectrometer, and the chemical shifts were reported relative to residual protonated solvent resonances. $^{31}\text{P}\{^1\text{H}\}$ spectra were recorded on a Bruker AC 300 MHz spectrometer, and the chemical shifts were reported relative to external standards H_3PO_4 (85%). HRMS data were recorded with the mass spectrometer Bruker Daltonics ICR-FTMS APEX II or with a Vg Analytical 7070 EQ. Steady-state emission and excitation spectra were measured using a Horiba scientific FluoroLog 3. The room temperature luminescence emissions of complex 7 were collected in dichloromethane (DCM) solution deaerated under argon bubbling. Low temperature measurements were carried out in 2-methyl tetrahydrofuran frozen glass at 77 K.

Monoborane Adduct (4). A solution of *n*BuLi (1.6 M in hexane, 0.772 mL, 1.234 mmol, 1.5 equiv) was added dropwise to a stirring solution of 1 (400 mg, 0.823 mmol) in dry THF (20 mL) at -78°C under a nitrogen atmosphere. The solution was stirred for 30 min at -78°C . The resulting yellow solution was treated with Ph_2PCl (0.221 mL, 1.234 mmol, 1.5 equiv) at -78°C , and the progress of the reaction was monitored by TLC (hexane/ CH_2Cl_2 , 7:3). After 5 h at -78°C , the yellow solution was warmed to 0°C and treated with a solution of $\text{BH}_3\cdot\text{THF}$ (1 M in THF, 8.23 mL, 8.23 mmol, 10 equiv). The yellow suspension was stirred for 30 min at 0°C , and then warmed to ambient temperature overnight. The suspension was slowly added to a saturated aqueous NH_4Cl solution (50 mL), and the aqueous phase was extracted with CH_2Cl_2 (4×20 mL). The organic phase was washed with water (2×20 mL), dried with Na_2SO_4 , and concentrated under reduced pressure. The crude product was purified by chromatography on silica gel (hexane/ CH_2Cl_2 , 7:3) to give 4 as pale yellow solid. Yield: 70% (394 mg, 0.576 mmol). The spectral properties of this compound were in agreement with those previously reported.¹⁹

Monophosphine (2). A suspension of 4 (50 mg, 0.073 mmol) in a mixture of EtOH/THF (7:4) (25 mL) was stirred and heated to reflux (the suspension became a yellow solution when hot) under an argon atmosphere, and the progress of the reaction was monitored by ^{31}P NMR analysis. After 4 h, the yellow solution was cooled to room temperature, and the solvents along with triethyl borate were removed under reduced pressure at 50°C to afford 2 as pale yellow solid. Yield: 98% (48 mg, 0.071 mmol). The spectral properties of this compound were in agreement with those previously reported.¹⁹

Diphosphine (3). A solution of 5 (120 mg, 0.136 mmol), in a mixture of EtOH/THF (2:1) (50 mL) was stirred and heated to reflux under an argon atmosphere, and the progress of the reaction was monitored by ^{31}P NMR analysis. After 3 h, the yellow solution was cooled to room temperature, and the solvents together with triethyl borate as byproduct were removed under reduced pressure at 50°C to afford 3 as yellow solid. Yield: 98% (115 mg, 0.134 mmol). The spectral properties of this compound were in agreement with those previously reported.¹⁹

Mononuclear Gold(I) Complex (6). To a solution of 2 (40.0 mg, 0.059 mmol, 1 equiv) in dry and degassed CH_2Cl_2 (3 mL) was added $\text{Au}(\text{tht})\text{Cl}$ (18.7 mg, 64.6 μmol , 1 equiv) under an argon atmosphere. The resulting yellow solution was stirred at room temperature for 1 h, and then the solvent was removed under reduced pressure to afford 6 as pale yellow powder. Yield: 99% (52 mg, 0.059 mmol). Mp 150°C (dec). ^1H NMR (CDCl_3 , 600 MHz): δ = 1.16 (m, 6 H), 1.85 (m, 4 H), 3.07 (m, 2 H), 3.13 (m, 2 H), 6.72 (d, J = 5.5 Hz, 1 H), 7.00 (d, J = 5.5 Hz, 1 H), 7.19 (d, J = 10.1 Hz, 1 H), 7.25 (m, 2 H), 7.33 (m, 6 H), 7.43 (m, 1 H), 7.48 (m, 1 H), 7.94 (m, 2 H), 8.06 (m, 2 H) ppm. $^{13}\text{C}\{^1\text{H}\}$ NMR (CDCl_3 , 150 MHz): δ = 14.67 (s, CH_3), 14.71 (s,

CH₃), 23.2 (s, CH₂, 2 C), 34.35 (s, CH₂), 34.38 (s, CH₂), 119.0 (s, CH), 120.2 (s, CH), 121.2 (s, CH), 122.4 (s, CH), 124.5 (s, CH), 125.2 (s, CH), 127.4 (s, C_q), 127.9 (d, ¹J_{C,P} = 62.8 Hz, C_q), 128.2 (s, C_q), 128.8 (d, ¹J_{C,P} = 64.1 Hz, C_q), 129.00 (d, ¹J_{C,P} = 64.8 Hz, C_q), 129.01 (d, ³J_{C,P} = 12.3 Hz, CH), 129.04 (d, ³J_{C,P} = 12.3 Hz, CH), 130.6 (s, C_q), 131.86 (d, ⁴J_{C,P} = 2.3 Hz, C_q), 131.9927 (s, C_q), 131.9944 (d, ⁴J_{C,P} = 2.3 Hz, C_q), 132.09 (s, C_q), 133.0 (s, C_q), 133.5 (d, ²J_{C,P} = 14.4 Hz, CH), 133.7 (d, ²J_{C,P} = 14.3 Hz, CH), 135.2 (s, C_q), 135.5 (d, ³J_{C,P} = 13.3 Hz, C_q), 136.5 (s, C_q), 136.7 (s, C_q), 136.8 (d, ²J_{C,P} = 14.0 Hz, CH), 136.9 (s, C_q), 140.0 (s, C_q), 140.1 (s, C_q), 141.7 (d, ⁴J_{C,P} = 5.1 Hz, C_q) ppm. ³¹P NMR (CDCl₃, 121 MHz): δ = 22.3 (s) ppm. MS (FAB⁺): *m/z* (%) = 902 (20) [M]⁺, 867 (100) [M - Cl]⁺. HRMS (EI): calcd for C₆₀H₅₂S₄PClAu 902.0400; found 902.0434.

Dinuclear Gold(I) Complex (7). To a solution of **3** (110 mg, 0.129 mmol, 1 equiv) in dry and degassed CH₂Cl₂ (3 mL) was added Au(tht)Cl (82.73 mg, 0.258 mmol, 2 equiv) under an argon atmosphere. The resulting yellow solution was stirred at room temperature for 1 h, and then the solvent was removed under reduced pressure to afford **7** as yellow crystals. Yield: 99% (168 mg, 0.128 mmol). Mp 310–311 °C (dec). ¹H NMR (CDCl₃, 600 MHz): δ = 1.15 (t, *J* = 7.3 Hz, 6 H), 1.85 (m, 4 H), 3.08 (m, 2 H), 3.14 (m, 2 H), 7.10 (m, 4 H), 7.15 (d, *J* = 10.2 Hz, 2 H), 7.21 (m, 4 H), 7.36 (m, 2 H), 7.42 (m, 8 H), 7.55 (m, 2 H), 8.05 (d, *J* = 8.6 Hz, 2 H), 8.09 (d, *J* = 8.6 Hz, 2 H) ppm. ¹³C{¹H} NMR (CDCl₃, 150 MHz): δ = 14.7 (s, CH₃, 2 C), 23.3 (s, CH₂, 2 C), 34.4 (s, CH₂, 2 C), 121.2 (s, CH, 2 C), 122.3 (s, CH, 2 C), 127.4 (s, C_q, 2 C), 128.2 (d, ¹J_{C,P} = 61 Hz, C_q, 2 C), 128.6 (d, ¹J_{C,P} = 63 Hz, C_q, 2 C), 128.9 (d, ¹J_{C,P} = 63 Hz, C_q, 2 C), 129.0 (d, ³J_{C,P} = 12.1 Hz, CH, 4 C), 129.4 (d, ³J_{C,P} = 12.2 Hz, CH, 4 C), 130.8 (s, C_q, 2 C), 131.8 (d, ⁴J_{C,P} = 2.4 Hz, CH, 2 C), 132.4 (d, ⁴J_{C,P} = 2.3 Hz, CH, 2 C), 132.9 (s, C_q, 2 C), 133.2 (d, ²J_{C,P} = 14.6 Hz, CH, 4 C), 133.9 (d, ²J_{C,P} = 14.4 Hz, CH, 4 C), 135.0 (d, ³J_{C,P} = 13.9 Hz, C_q, 2 C), 136.2 (d, ²J_{C,P} = 14.7 Hz, CH, 2 C), 137.1 (s, C_q, 2 C), 140.3 (s, C_q, 2 C), 141.8 (d, ⁴J_{C,P} = 4.5 Hz, C_q, 2 C) ppm. ³¹P NMR (CDCl₃, 121 MHz): δ = 22.4 (s) ppm. MS (FAB⁺): *m/z* (%) = 1283 (100) [M - Cl]⁺, 1051 (48) [M - AuCl₂]⁺. HRMS (ESI): calcd for C₅₂H₄₀S₄P₂Cl₂Au₂Na (M⁺) 1341.0088; found 1341.0097. Anal. Calcd for C₅₂H₄₀S₄P₂Cl₂Au₂ (M_w 1318.1): C, 47.32; H, 3.05. Found: C, 47.04; H, 3.29. Yellow crystals of **7** for X-ray diffraction were grown from CH₂Cl₂/hexane mixture at room temperature over a period of several hours.

General Procedure for Gold-Catalyzed Reactions. The specific substrate and the internal standard were dissolved in deuterated solvent, and an NMR spectrum was measured. Catalyst **6** or **7** together with AgNTf₂ or AgOTf was added, and the tube was shaken vigorously at room temperature. The yield of the products was determined by integrating the NMR signals against the internal standard.

For entries 1–3 of Table 5, the following conditions were used: **8** (30.0 mg, 200 μmol), tri-*tert*-butylbenzene (2 mg, internal standard), CDCl₃ (500 μL), **6** or **7**, and AgNTf₂ (0.5–4 μmol, 0.25–2 mol %, a 1 wt % solution in CDCl₃). Yield of **9**: 4–23%.

For entries 4–5 of Table 5, the following conditions were used: **10** (42.0 mg, 200 μmol), tri-*tert*-butylbenzene (2 mg, internal standard), CD₂Cl₂ (500 μL), **6** or **7**, and AgNTf₂ (4 μmol, 2 mol %, a 1 wt % solution in CD₂Cl₂). Yield of **11**: 15–30%. Yield of **12**: 5–20%.

For entries 6–8 of Table 5, the following conditions were used: **13** (41.6 mg, 125 μmol), hexamethylbenzene (2 mg, internal standard), CD₂Cl₂ (500 μL), **6** or **7**, and AgNTf₂ (1.25–6.25 μmol, 2 mol %, a 1 wt % solution in CD₂Cl₂). Yield of **14**: 65–99%.

For entry 9 of Table 5, the following conditions were used: **15** (12.8 mg, 100 μmol), CHCl₃ (internal standard), C₆D₆ (500 μL), **7** (2.5 mol %), and AgOTf (5 mol %). Yield of **16**: 99%.

X-ray Crystallographic Analysis for compound 7. Data for the X-ray crystallographic analysis of **7** were collected on a Bruker Smart CCD diffractometer (Mo Kα radiation, λ = 0.710 73 Å). Crystallographic and experimental details are summarized in Table 1. The structure was solved by direct methods and refined against *F*² with full-matrix least-squares algorithm using the software package SHELXTL 2008/1 for structure solution and refinement.²²

Table 1. Crystallographic Data for Compound 7

formula	C _{52.50} H ₄₁ Au ₂ Cl ₃ P ₂ S ₄ (7)
mol wt	1362.32
<i>T</i> , K	200(2)
crystal syst	monoclinic
space group	<i>P</i> 2 ₁ / <i>c</i>
<i>a</i> , Å	12.3030(1)
<i>b</i> , Å	30.9040(1)
<i>c</i> , Å	12.8265(1)
α, deg	90
β, deg	90.411(1)
γ, deg	90
<i>V</i> , Å ³	4876.66(6)
<i>Z</i>	4
<i>D</i> _{calcd} , g cm ⁻³	1.86
<i>F</i> (000)	2636.0
cryst size (mm ³)	0.11 × 0.10 × 0.08
μ, mm ⁻¹	6.45
reflns collected	48 434
reflns unique	11 131 (<i>R</i> _{int} = 0.0575)
reflns obsd [<i>I</i> > 2σ(<i>I</i>)]	8717
params	596
<i>R</i> indices [<i>I</i> > 2σ(<i>I</i>)] ^a	<i>R</i> 1 = 0.039, <i>wR</i> 2 = 0.073
<i>R</i> indices (all data)	<i>R</i> 1 = 0.0610, <i>wR</i> 2 = 0.0798

$$^a R1 = \sum ||F_o| - |F_c|| / \sum |F_o|. \quad wR2 = [\sum [w(F_o^2 - F_c^2)^2] / \sum [w(F_o^2)^2]]^{1/2}.$$

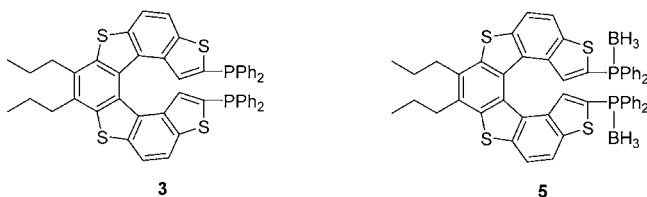
Quantum Chemical Calculations. The equilibrium structures of the ground states of compounds **3**, **5**, and **7** have been optimized at the theoretical level of density functional theory (DFT)²³ using the long-range separated exchange-correlation (xc) functional ωB97X,²⁴ the 6-31G* basis set for the light atoms, and the LANL2DZ effective core potential for gold as implemented into Gaussian09 Rev. A02.²⁵ The lowest excited states of these compounds have been computed with time-dependent DFT (TDDFT)²⁶ employing the same xc-functional basis set combination. An evaluation of xc-functionals with varying amounts of nonlocal Hartree–Fock (HF) exchange has demonstrated that at least 50% are required to avoid the occurrence of spurious low-lying charge-transfer excited states and to achieve a reasonable agreement with the experimental spectra. Here, ωB97X has turned out to yield the most reliable results and to be required for reliable excited state geometry optimizations.²⁷ However, the high amount of HF exchange leads to an essentially constant shift of the computed spectra to higher excitation energies as compared to the experimental ones.²⁸ For the interpretation of the fluorescence spectrum of **7** the equilibrium structures of the two lowest singlet S₁ and S₂ states have been optimized. The properties of the compounds **3** and **5** were computed for the gas phase only, while for **7**, the calculations were performed in combination with a polarizable continuum model (C-PCM) for dichloromethane solution.²⁹ While all optimizations have been performed using equilibrium solvation, electronic transitions are computed with its nonequilibrium counterpart. In general it turned out that modeling DCM solvation has only a negligible effect on structures and spectra of compound **7**.

■ RESULT AND DISCUSSION

Improvement on the Selective Synthesis of Mono Adduct 4. Since diphosphane **3** is easily oxidized by the oxygen of air, we developed an efficient one-pot procedure to prepare the corresponding air-stable borane adduct **5**, which could be readily converted into the free phosphane **3** (Chart 3).¹⁹

On the contrary, the first studies aimed at preparing monoborane adduct **4**, from which the free monophosphane **2** can be recovered, gave unsatisfactory results in terms of yield and selectivity. In fact, the reaction between helicene **1** with **2**

Chart 3



equiv of *n*BuLi and Ph_2PCl , followed by the addition of an excess of $\text{BH}_3\cdot\text{THF}$, provided the monoborane **4** in 39% yield together with the diborane **5** in 49% yield.¹⁹ We found that the selectivity toward the formation of monoborane **4** can be much improved by using the proper amount of base and chlorodiphenylphosphine. In particular, the use of 1.5 equiv of *n*BuLi and 1.5 equiv of Ph_2PCl provided the mono adduct **4** in 70% yield, together with only a 10% of unreacted helicene **1**, and no disubstituted borane adduct **5** was observed in the crude reaction mixture (Scheme 1).

Both monoborane and diborane adduct **4** and **5** can be quantitatively converted into the corresponding free mono- and diphosphane **2** and **3**, respectively, by heating to reflux in a mixture of MeOH or EtOH and THF under an inert atmosphere.^{19,30}

Synthesis of Mono- and Dinuclear Au(I) Complexes 6 and 7. Exploiting this general and reliable synthetic procedure to prepare 7-TH mono- and diphosphane ligands for transition metals, we focused our attention on the synthesis of the new mono- and dinuclear gold(I) complexes **6** and **7** in view of their potential applications in optoelectronics as well as in homogeneous catalysis.

Phosphinogold(I) chloride complexes are most commonly prepared by substitution reaction of the weakly coordinated tetrahydrothiophene (tht) in $\text{Au}(\text{tht})\text{Cl}$ with an appropriate phosphine. Therefore, mono- and diphosphane **2** and **3** were reacted with 1 and 2 equiv of $\text{Au}(\text{tht})\text{Cl}$, respectively, in CH_2Cl_2 at room temperature for 1 h (Scheme 2).

Evaporation of the solvent afforded air-stable yellow solids **6** and **7** in nearly quantitative yields. The complexes were fully characterized by means of analytical and spectroscopic analyses whose results were consistent with the proposed structures for these compounds. In particular, the $^{31}\text{P}\{^1\text{H}\}$ NMR spectra of **6** and **7** display one sharp singlet at $\delta +22$ ppm, that is a value comparable with those found in other gold(I) complexes with mono- and diphenyl phosphines.^{5d} Coordination to Au(I) produced the expected downfield shift (*ca.* 40 ppm) with respect to the free phosphanes **2** and **3** (−15 ppm). FAB mass spectra of **6** and **7** gave the corresponding parent peak at *m/z* 867 and 1283, respectively, attributable to the molecular ions resulting from loss a chlorine atom $[\text{M} - \text{Cl}]^+$. These results are consistent with one gold center per ligand in complex **6** and two gold centers per ligand in complex **7**. As described below,

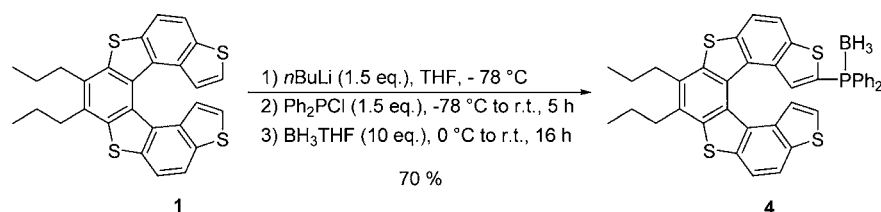
the structure of dinuclear complex **7** was also fully elucidated by X-ray crystal structure analysis, while we have been unable to obtain suitable single crystals for the mononuclear complex **6**, which was significantly less soluble in the organic solvents than complex **7**. Finally, taking into account that diphosphane **3** was able to generate chelate monodentate complexes with Rh(I) salts,¹⁹ many efforts have been carried out to synthesize a chelate monodentate gold(I) complex by reacting **3** with $\text{Au}(\text{tht})\text{Cl}$ in 1:1 molar ratio. Unlike Rh(I) salts, $\text{Au}(\text{tht})\text{Cl}$ afforded no chelate complex with **2**. Presumably, this is due to the too large P–P distance (up to 5 Å) between the two PPh_2 groups in the helical structure of **3**, in combination with the great tendency of gold(I) centers to form linear two-coordinate complexes.

Crystal Structure of Dinuclear Complex 7. Polyhedron yellow crystals of dinuclear complex **7** were grown from layered CH_2Cl_2 /hexane, and its solid-state structure was determined by X-ray crystallography. The structure of **7** consists of a pair of AuCl bridged by one bis(phosphine)ligand as shown in Figure 1. Binuclear gold(I) complexes are commonly found with bidentate phosphine ligands. The gold(I) centers do not interact with the thiophene moieties, demonstrating their strong preference for phosphine donors.³¹ The high values of intra- and intermolecular distances between gold(I) atoms and the thiophene sulfur atoms indicate no bonding interaction. On the other hand, theoretical investigations³² along with experimental studies³³ on the interactions between thiophene rings and gold(I) centers are in agreement with our results.

Compound **7** crystallizes in space group $P2_1/c$ with one-half of a molecule of CH_2Cl_2 in the asymmetric unit, and both enantiomers are present in the crystal.

In Table 2 selected bond lengths and angles for **7** are reported, and there are no unusual features of the gold coordination geometry while some distortions are found in the helical system. The Au–Cl bond lengths [2.30 and 2.28 Å] are longer than the P–Au bonds [2.24 and 2.23 Å], and fall within the expected range for other related phosphinogold(I) halide complexes. The P–Au–Cl fragments are nearly linear with angles of 175.4° and 172.4°, and they are almost perpendicular to each other, with absolute value of Cl–Au⋯Au–Cl torsion angle of 93°. The most striking feature of this complex is the Au⋯Au distance of 3.18 Å, which indicates a moderate intramolecular aurophilic interaction. Such interactions are common in the gold(I) chemistry, and, in this case, could be accountable for the unusual small value of 45° of the total dihedral angle between the two terminal thiophene rings. In fact, unsubstituted helicene **1** shows a total dihedral angle of 53°, and 2,13-disubstituted helicenes, for example with bulky alkyl silyl groups, display much higher angles (up to 59°).³⁴ However, all of the seven fused rings show distortion from planarity, and the dihedral angles between adjacent rings increases passing from the “external” thiophene rings to the

Scheme 1. Synthesis of Monoborane Adduct 4



Scheme 2. Synthesis of Au(I) Complexes 6 and 7

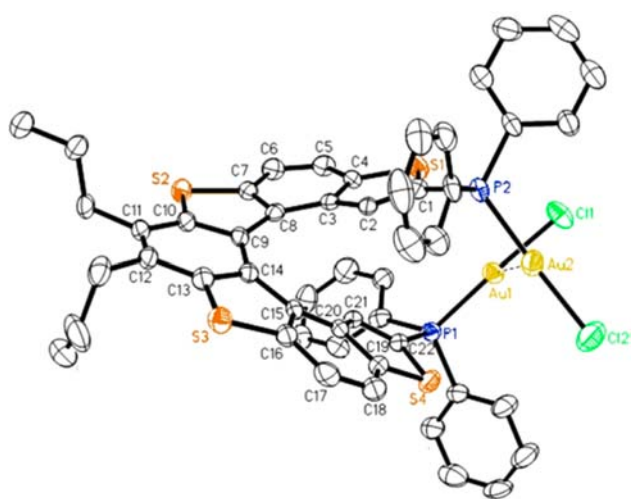
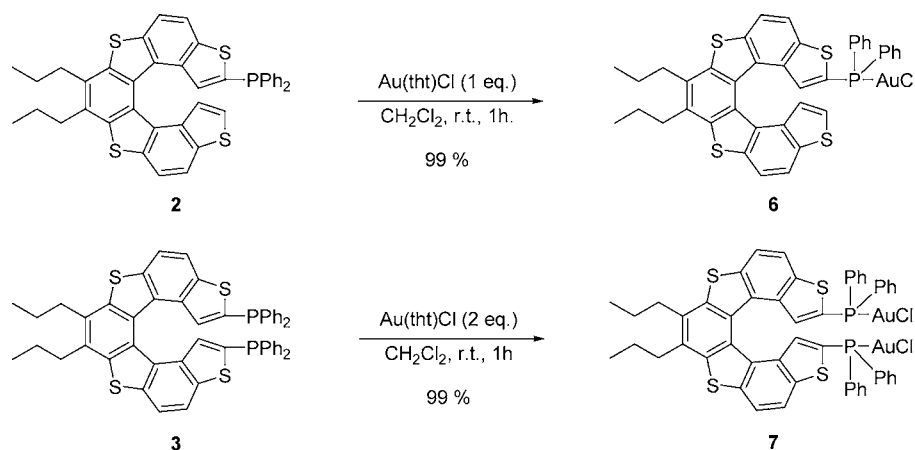


Figure 1. ORTEP view of dinuclear complex 7. Hydrogen atoms are omitted for clarity, and thermal ellipsoids are drawn at 50% probability.

Table 2. Selected Bond Lengths and Angles for 7

Distances, Å			
Au(1)–P(1)	2.2438(14)	C(5)–C(6) outer	1.360(8)
Au(2)–P(2)	2.2317(14)	C(8)–C(9) inner	1.449(7)
Au(1)–Cl(1)	2.3078(14)	C(11)–C(12) outer	1.396(8)
Au(2)–Cl(2)	2.2868(16)	C(15)–C(20) inner	1.423(7)
Au(1)–Au(2)	3.1825(3)	C(17)–C(18) outer	1.364(8)
C(2)–C(3) inner	1.429(7)	C(20)–C(21) inner	1.436(7)
C(3)–C(8) inner	1.418(7)	C(9)–C(14) inner	1.428(7)
Angles, deg			
P(1)–Au(1)–Cl(1)	175.44(5)	Cl(2)–Au(2)–Au(1)	93.78(5)
P(2)–Au(2)–Cl(2)	172.40(6)	C(22)–P(1)–Au(1)	112.90(17)
P(2)–Au(2)–Au(1)	93.82(4)	C(1)–P(2)–Au(2)	115.29(17)

“central” benzene ring of the helicene. Finally, the outer core C–C bond lengths of 7 are shorter and those of the inner core are longer than the normal value of 1.39 Å, in common with similar compounds,^{19,34,35} implying a lower π character for the inner-core C–C bonds and a higher π character for the outer-core ones (i.e., higher π electron density along the periphery of the molecule).

Photoluminescence Studies on Complex 7. The luminescence displayed by Au(I) complexes is an interesting

property. The origin of Au(I) complexes' optical (absorption–emission) behaviors has been ascribed to different types of electronic transitions. These include the limiting situations of electronic transitions between metal centered states (MC) or between ligand centered states (LC)^{36a} according to the nature of the phosphine,^{9,36b,c} and/or the presence of metal–metal cluster interaction.³⁷

The gold(I) complex 7 shows luminescence emission both in diluted room temperature solution as well as in the solid state. For sake of comparison, the absorption and luminescence features of 7 have been compared with those collected for the phosphino-borane adduct 5. Adduct 5 has been chosen as suitable reference chromophore since it is air-stable (contrarily to the free phosphine 3),¹⁹ and the electronic environment surrounding the P atoms is the same as in the metal complex 7 (i.e., the P lone pair is employed to coordinate a boron atom or the gold one).

The preliminary results of this study are depicted in Figures 2 and 3. Figure 2 reports the absorption (inset), emission, and

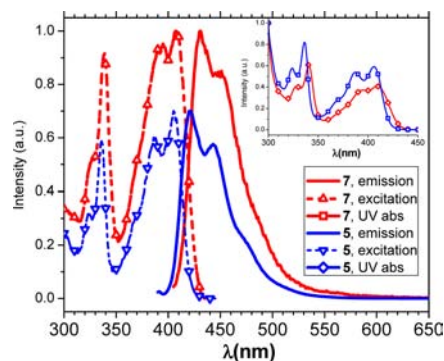


Figure 2. Normalized room temperature emission (straight lines) and excitation (dashed lines) spectra of compounds 5 and 7 in DCM solution (the solution of 7 was deaerated with argon bubbling).

excitation profiles of 7 and 5 at room temperature in deaerated dichloromethane solution, along with the observed emissions at 77 K in the rigid 2-MeTHF glass.

The UV–vis absorption spectra of 5 and 7 (inset Figure 2) closely resemble each other, with 7 only 6 nm red-shifted compared to 5. This is due to the presence of the gold atoms. In both systems, the UV absorptions are characterized by a low energy (350–420 nm) IL transition of HOMO to LUMO

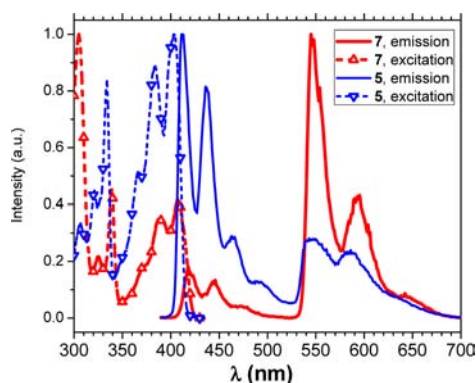


Figure 3. Normalized emission (straight lines) and excitation (dashed lines) spectra of compounds **5** and **7** at 77 K in 2-MeTHF rigid glass.

($\pi-\pi^*$) character.^{38,17b} This implies that, together with the similar UV-vis shape, the 7-TH phosphine chromophore dominates the optical feature of the gold derivative **7**.

Complex **7** emits at 430 nm in diluted solution at room temperature (red line, Figure 2), and the corresponding excitation profile (dashed red line) matches the electronic absorption spectra (inset Figure 2) already described. In the same conditions, the borane adduct **5** (blue line) fluoresces at 420 nm. Therefore, it should be concluded that the 430 nm emission of **7** could be attributed to the IL fluorescence of 7-TH slightly perturbed by the presence of Au(I) atoms.

In rigid 2-MeTHF at 77 K, complex **7** displays two set of emissions at 400–500 and 530–700 nm (Figure 3). The weak fluorescence emission at 418 nm, due to rigidochromic effect, is slightly blue-shifted compared to the room temperature fluorescence (430 nm), and it is characterized by a well-resolved vibronic progression with breathing mode of about 1500 cm^{-1} . The low energy bands between 530 and 700 nm and peaked at *ca.* 577 nm are characterized by vibronic progression of about 1400 cm^{-1} . These bands are attributed to the phosphorescence emission of the aromatic helicene scaffold, since they closely overlay to the bands observed in the same region for borane **5** (blue line). Worth noting, compared to **5**, the overall 77 K emission of **7** differs in two significant parameters, that are consequences of the presence of the Au atoms: (a) the relative phosphorescence vs fluorescence intensity ratio is higher in **7** than that in **5**; (b) the phosphorescence lifetime of **7** is at least 1 order of magnitude shorter than that in **5** ($\tau_4 \sim 0.12\text{ s}$).

Both observations are the consequence of the so-called “heavy atom effect”, due to the gold atoms through the indirect spin orbit coupling (SOC).³⁹

Au(I) modulates the overall photophysical kinetics in **7**, increasing both the rate of intersystem crossing (ISC) from the first excited singlet state to the excited triplet one, and the radiative rates of the phosphorescence emission.

The room temperature solid state emission of **7** is reported in Figure 4, together with the 77 K data collected on the same sample. In the solid state, **7** displays a broad featureless fluorescence between 420 and 600 nm (blue line). Upon cooling the same sample at 77 K (red line), the fluorescence emission gains a slight structured vibronic progression, and phosphorescence emission appears (560–700 nm). This “thermochromic effect”^{36a} might point to the presence of energetically close and accessible deactivating states, thermally

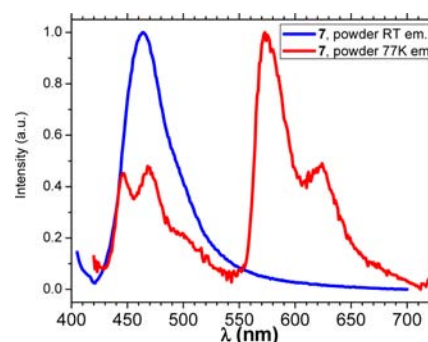


Figure 4. Normalized emission spectra of the solid **7** at room temperature and at 77 K.

populated at room temperature and not accessible at low temperature.

Quantum Chemical Calculations. The equilibrium structures of the S_0 , S_1 , S_2 , and T_1 electronic states of **7** have been separately optimized, and selected geometrical parameters are compiled in Table 3. As can be readily seen, the computed

Table 3. Selected Computed Bond Lengths and Angles for **7** Optimized in the Electronic Ground State S_0 , the First and Second Excited Singlet States S_1 and S_2 , and in the Lowest Triplet State T_1

	S_0	S_1	S_2	T_1
Distances (Å)				
Au(1)–P(1)	2.305	2.308	2.307	2.306
Au(2)–P(2)	2.307	2.310	2.309	2.308
Au(1)–Cl(1)	2.389	2.393	2.392	2.391
Au(2)–Cl(2)	2.391	2.394	2.394	2.391
Au(1)–Au(2)	3.320	3.309	3.312	3.322
C(2)–C(3) inner	1.440	1.422	1.431	1.428
C(3)–C(8) inner	1.422	1.438	1.423	1.443
C(5)–C(6) outer	1.376	1.397	1.398	1.395
C(8)–C(9) inner	1.463	1.408	1.434	1.390
C(11)–C(12) outer	1.391	1.449	1.409	1.489
C(15)–C(20) inner	1.425	1.439	1.424	1.434
C(17)–C(18) outer	1.376	1.394	1.397	1.382
C(20)–C(21) inner	1.440	1.424	1.431	1.435
C(9)–C(14) inner	1.423	1.454	1.417	1.478
Angles, deg				
P(1)–Au(1)–Cl(1)	176.4	176.6	176.3	176.6
P(2)–Au(2)–Cl(2)	176.6	176.2	176.3	176.2
P(2)–Au(2)–Au(1)	98.1	96.8	97.9	97.8
Cl(2)–Au(2)–Au(1)	85.2	86.8	85.7	85.9
C(22)–P(1)–Au(1)	112.6	113.6	113.4	112.9
C(1)–P(2)–Au(2)	113.3	114.7	114.2	114.0

values for the electronic ground state S_0 agree very nicely with those determined by X-ray analysis (Table 2). The largest deviations of approximately 0.1 Å occur for the bond where the gold atoms are involved. In particular, the computed Au–Au distance is found to be slightly larger with 3.32 Å as compared to the experimental value of 3.18 Å . Most likely this deviation is due to the use of a rather small basis set and an effective core potential for the gold atoms. All other bond lengths deviate by less than 0.1 Å . The largest deviations in the bond angles is found for the P(2)–Au(2)–Au(1) and Cl(2)–Au(2)–Au(1) angles. Here, in addition to the limited basis set size also crystal

packing effects may play a role, which are not included in the calculations.

At the optimized S_0 equilibrium geometry, the lowest excited singlet states S_1 to S_4 have been computed including the continuum effects of DCM solvation (Table 4). All these states

Table 4. Excitation Energies and Oscillator Strengths of the Four Lowest Excited Singlet States of 7 at the Calculated Equilibrium Structures of S_0 , S_1 , and S_2 at the Level of TDDFT/ ω B97X/6-31G*

state	S_0	S_1	S_2
S_1	3.81 (0.22)	3.03 (0.38)	3.46 (0.32)
S_2	3.94 (0.38)	3.55 (0.66)	3.52 (0.62)
S_3	4.45 (0.22)	4.12 (1.01)	4.26 (0.44)
S_4	4.50 (0.68)	4.18 (0.46)	4.28 (0.93)

correspond to typical $\pi\pi^*$ excited states located on the tetrathiahelicene ligand. In particular, S_1 and S_2 correspond to typical electronic transitions from the highest occupied molecular orbital (HOMO) and HOMO – 1 into the lowest unoccupied molecular orbital (LUMO) (Figure 5). S_3 and S_4 are not easily described within the molecular orbital picture, since they correspond to mixtures of several electronic transitions. However, analysis of the transition densities reveals their $\pi\pi^*$ character. According to our calculations, S_1 and S_2 are only slightly energetically separated (Table 3) and could both be contained in the first peak of the experimental spectrum. The energy spacing between the vertical excitation energies is only 0.12 eV.

The similarity of the electronic structures of the excited S_1 and S_2 states is further confirmed by their closely related equilibrium structures. By analyzing the geometrical parameters (Table 3) only marginal differences can be identified. Most strikingly, for all considered states, the geometrical parameters in the vicinity of the gold atoms do hardly change upon excitation of 7, which also demonstrates that orbitals at the gold atoms are not involved in the low-lying excited states of 7. Of course, the vertical excitation energies decrease upon geometry relaxation, and the S_1 state exhibits an excitation energy of only 3.03 eV at its equilibrium geometry, which can be compared to the fluorescence wavelength of 430 nm (2.9 eV). The phosphorescence wavelength of 7 can be computed as energy difference between the total energies of the optimized S_0 structure and optimized T_1 structure both obtained at DFT/ ω B97X level. Here we find an energy difference of 2.58 eV

compared to the experimental phosphorescence wavelength of 545 nm (2.27 eV). In general, one can not expect a better agreement, since the computed vertical absorption, fluorescence, and phosphorescence energies are given as energy differences of the electronic surfaces only, while the peaks in the spectra correspond to vibronic 0–0 transitions.

For comparison, also the energetically lowest excited states of the free ligands 3 and 5 have been computed. They exhibit practically identical excitation energies and oscillator strengths as gold complex 7. In analogy, they correspond to $\pi\pi^*$ excited state with the same frontier orbital structure. Hence, it is safe to conclude that the photoluminescence properties can be attributed to the tetrathiahelicene ligand only, with the gold atoms inducing only a “heavy atom” effect on the phosphorescence quantum yield without largely changing the electronic structure of the involved states.

Catalysis Study. Having secured good access to mono- and dinuclear gold(I) complexes 6 and 7, respectively, we then explored the possibility of using them as new catalysts in the field of the homogeneous gold catalysis. In particular, we selected four different gold(I)-catalyzed cycloisomerizations as screening reactions for new catalysts, and the results of this study are listed in Table 5.

Thanks to the diamagnetic character of gold(I), all experiments were performed in an NMR tube, and then monitored by ^1H NMR analysis. The electrophilic gold(I) active species $[\text{AuL}]^+$ in the catalytic activation of alkynes or allenes are often formed by chloride abstraction from $[\text{AuCl}(\text{L})]$ complexes using silver(I) salts.⁴⁰ In our test reactions, complexes 6 and 7 were converted into the active catalysts *in situ* by removal of the chloride with a silver salts (AgNTf_2 or AgOTf) of a noncoordinating counterion. Catalysts 6 and 7 were then tested in the cyclization of ω -alkynylfuran 8⁴¹ (entries 1–3), the cyclization of 1,6-enyne 10⁴² (entries 4–5), and the intramolecular hydroarylation of allene 13⁴³ (entries 6–8), and catalyst 7 was also tested in the hydroxycarboxylation of allene-carboxylate 15⁴⁴ (entry 9). As reported in Table 5, gold(I) complexes 6 and 7 have been shown to be ineffective catalysts for the cyclization of ω -alkynylfuran 8 to give phenol 9, which was obtained in 18% and 4% yield, using 0.25 mol % of 6 and 7, respectively (entries 1 and 2). Increasing the catalyst loading of 7 to 2 mol %, the yield of 9 did not significantly improve (entry 3). Slightly better results in terms of yield were obtained in the isomerization reaction of 1,6-enyne 10 (entries 4 and 5). However, the use of 2 mol % of both catalysts 6 and 7 yielded a mixture of cyclohexene

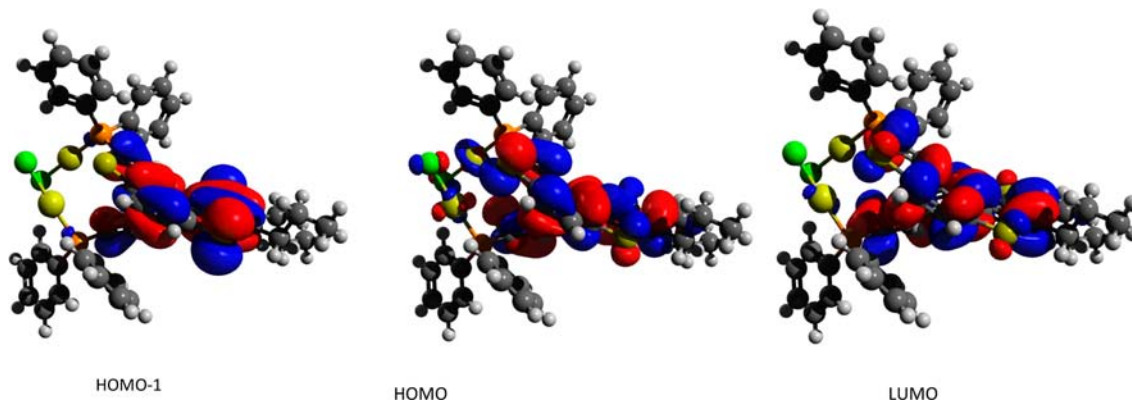
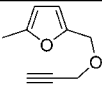
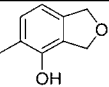
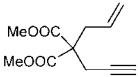
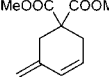
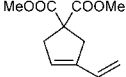
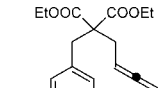
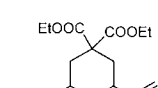
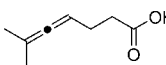
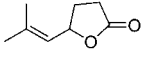


Figure 5. Frontier molecular orbitals of 7 involved in the two lowest excited electronic states S_1 and S_2 .

Table 5. Gold(I)-Catalyzed Cyclizations with **6** and **7**

Entry ^[a]	Reactants	Products	Catalyst ^[b] (mol %)	Conversion [%] ^[c]	Yield [%] ^[c]	
1			6 (0.25)	88	18	
2	8	9	7 (0.25)	94	4	
3	8	9	7 (2)	100	23	
4				6 (2)	25	15 (11) and 5 (12)
5	10	11	12	7 (2)	55	30 (11) and 20 (12)
6			6 (5)	100	99	
7	13	14	6 (1)	67	65	
8	13	14	7 (5)	94	99	
9 ^[d]			7 (2.5)	100	99	

^aThe reactions were performed in NMR tubes at room temperature. Before adding the catalyst, an NMR spectrum was measured. ^bUnless otherwise indicated, equimolar amounts of AgNTf₂ were added together with the catalysts **6** and **7**. ^cDetermined by integration and comparison with an internal standard. ^d5 mol % of AgOTf was added together with catalyst **7**.

derivative **11** and vinyl cyclopentene **12** in scarce regioselectivity, with the diene **11** as the major isomer. In the case of catalyst **6** the selectivity is slightly better (**11**:**12** = 3:1), but the conversion and yield are lower (entry 4), while in the case of the more reactive **7** (conversion and combined yield is higher) the selectivity is lower (**11**:**12** = 3:2, entry 5). The selectivity toward the formation of **11** was also observed in the cycloisomerization of enyne **10** using Au(PPh₃)Cl/AgSbF₆ as catalyst system, although in this case the selectivity in favor of diene **11** was much higher.^{42a}

On the contrary, **6** and **7** both proved to be highly efficient catalysts in the intramolecular allene hydroarylation reactions (entries 6–8), and in the hydroxycarboxylation of allenecarboxylate **15** (entry 9). In particular, both **6** and **7** efficiently react with 4-allenyl arene **13** in an *exo* fashion to provide the corresponding vinylbenzocycle **14** in excellent yield (99%, entries 6 and 8). On the other hand, a good yield of product **14**

was also obtained when the catalyst loading of **6** was reduced from 5 to 1 mol % (65%, entry 7). Finally, the cyclization of the carboxylate **15** in the presence of 2.5 mol % of gold(I) phosphine **7** in combination with 5 mol % of AgOTf gave the corresponding lactone **16** in almost quantitative yield (entry 9). This result is very similar to that previously reported in the cyclization of **15** using 2.5 mol % of [dppm(AuCl)₂] activated with 5 mol % of silver salt, in which **16** was obtained in 91% yield.⁴⁴

CONCLUSION

In this Article, we have reported the synthesis and the characterization of new gold(I) complexes **6** and **7** with phosphanes **2** and **3**, respectively, which represent the first example of gold complexes of phosphine based on the helicene scaffold. The molecular structure of dinuclear complex **7** was determined by X-ray diffraction analysis, showing an aurophilic

interaction, with the Au–Au bond distance of 3.18 Å, which could explain the unusual short value of 45° of the dihedral angle between the two terminal thiophene rings of the helical skeleton. First studies on the photophysical properties of **7** along with experiments on the use of **6** and **7** as catalysts in typical Au(I) cycloisomerization reactions have been also investigated. In particular, organophosphane–Au(I) complex **7** shows interesting luminescent properties, in solution as well as in the solid state, which are ascribed to both fluorescence and (only at 77 K) phosphorescence emission. Quantum chemical calculations demonstrate that the photophysical properties of **7** are determined by transitions between ligand centered states only (both singlet and triplet), slightly perturbed by the presence of gold atoms through the indirect spin orbit coupling (SOC). Finally, complexes **6** and **7** have been shown to be efficient catalysts in the intramolecular hydroarylation of allene **13**, and the hydroxycarboxylation of allene-carboxylate **15**. The enantiopure form of this new class of gold(I) complexes based on 7-TH phosphanes may find important applications in the field of the chiral nonlinear optical materials, as well as in the asymmetric catalysis.

AUTHOR INFORMATION

Corresponding Author

*E-mail: emanela.licandro@unimi.it (E.L.); hashmi@hashmi.de (A.S.K.H.).

Author Contributions

The manuscript was written through contributions of all authors. All authors have given approval to the final version of the manuscript.

Notes

The authors declare no competing financial interest.

ACKNOWLEDGMENTS

S.C. acknowledges the University of Milan for the postdoctoral fellowship. M.C.B.J. is grateful to the DAAD for a fellowship. Gold salts were generously donated by Umicore AG & Co. KG. This work was supported by the Ministero dell'Università e della Ricerca (MIUR) and the University of Milan, PRIN 2007 (prot. 2007XFA27F_004), PUR 2008.

ABBREVIATIONS; 7-TH, tetrathiahelicene; tht, tetrahydrothiophene; DCM, dichloromethane; FAB, fast atom bombardment; SOC, spin orbit coupling; 2-MeTHF, 2-methyl tetrahydrofuran; TLC, thin layer chromatography

REFERENCES

- (1) *Modern Gold Catalyzed Synthesis*; Hashmi, A. S. K., Toste, D. F., Eds.; Wiley-VCH: Weinheim, Germany, 2012.
- (2) *Gold: Progress in Chemistry, Biochemistry and Technology*; Schmidbaur, H., Ed.; John Wiley & Sons: Chichester, U.K., 1999.
- (3) (a) Berners-Price, S. J.; Filipovska, A. *Metallomics* **2011**, *3*, 863–873. (b) Shaw, C. F. *Chem. Rev.* **1999**, *99*, 2589–2600.
- (4) (a) Gómez-Suárez, A.; Nolan, S. P. *Angew. Chem., Int. Ed.* **2012**, *51*, 8156–8159. (b) Hashmi, A. S. K. *Angew. Chem., Int. Ed.* **2010**, *49*, 5232–5241. (c) Gorin, D. J.; Sherry, B. D.; Toste, F. D. *Chem. Rev.* **2008**, *108*, 3351–3378. (d) Arcadi, A. *Chem. Rev.* **2008**, *108*, 3266–3325. (e) Li, Z.; Brouwer, C.; He, C. *Chem. Rev.* **2008**, *108*, 3239–3265. (f) Hashmi, A. S. K. *Chem. Rev.* **2007**, *107*, 3180–3211. (g) Gorin, D. J.; Toste, F. D. *Nature* **2007**, *446*, 395–403. (h) Hashmi, A. S. K.; Hutchings, G. J. *Angew. Chem., Int. Ed.* **2006**, *45*, 7896–7936.
- (5) (a) Koshevoy, I. O.; Lin, C. L.; Hsieh, C. C.; Karttunen, A. J.; Haukka, M.; Pakkanen, T. A.; Chou, P. T. *Dalton Trans.* **2012**, *41*, 937–945. (b) He, X.; Yam, V. W. W. *Coord. Chem. Rev.* **2011**, *255*, 2111–2123. (c) Yam, V. W. W.; Cheng, E. C. C. *Chem. Soc. Rev.* **2008**, *37*, 1806–1813. (d) Pintado-Alba, A.; de la Riva, H.; Nieuwhuyzen, M.; Bautista, D.; Raithby, P. R.; Sparkes, H. A.; Teat, S. J.; López-de-Luzuriaga, J. M.; Lagunas, M. C. *Dalton Trans.* **2004**, 3459–3467.
- (6) (a) Wetzels, C.; Kunz, P. C.; Kassack, M. U.; Hamacher, A.; Böhrer, P.; Watjen, W.; Ott, I.; Rubbiani, R.; Spingler, B. *Dalton Trans.* **2011**, *40*, 9212–9220. (b) Tian, S. H.; Siu, F. M.; Kui, S. C. F.; Lok, C. N.; Che, C. M. *Chem. Commun.* **2011**, *47*, 9318–9320. (c) Scheffler, H.; You, Y.; Ott, I. *Polyhedron* **2010**, *29*, 66–69.
- (7) (a) Wang, F. J.; Liu, L. J.; Wang, W. F.; Li, S. K.; Shi, M. *Coord. Chem. Rev.* **2012**, *256*, 804–853. (b) Nolan, S. P. *Acc. Chem. Res.* **2011**, *44*, 91–100. (c) Marion, N.; Nolan, S. P. *Chem. Soc. Rev.* **2008**, *37*, 1776–1785. (d) Hashmi, A. S. K.; Lothschütz, C.; Böhring, C.; Hengst, T.; Hubbert, C.; Rominger, F. *Adv. Synth. Catal.* **2010**, *352*, 3001–3012. (e) Hashmi, A. S. K.; Riedel, D.; Rudolph, M.; Rominger, F.; Oeser, T. *Chem.—Eur. J.* **2012**, *18*, 3827–3830.
- (8) (a) Pradal, A.; Toullec, P. Y.; Michelet, V. *Synthesis* **2011**, 1501–1514. (b) Sengupta, S.; Shi, X. D. *ChemCatChem* **2010**, *2*, 609–619. (c) Widenhofer, R. A. *Chem.—Eur. J.* **2008**, *14*, 5382–5391. (d) Ito, Y.; Sawamura, M.; Hayashi, T. *J. Am. Chem. Soc.* **1986**, *108*, 6405–6406.
- (9) (a) Koshevoy, I. O.; Lin, C.-L.; Hsieh, C.-C.; Karttunen, A. J.; Haukka, M.; Pakkanen, T. A.; Chou, P.-T. *Dalton Trans.* **2012**, *41*, 937–945. (b) Pawlosky, V.; Kunkely, H.; Vogler, A. *Inorg. Chem. Acta* **2004**, *357*, 1309–1312. (c) Fife, D. J.; Morse, K. W.; Moore, W. M. J. *Photochem.* **1984**, *24*, 249–263.
- (10) Shen, Y.; Chen, C. F. *Chem. Rev.* **2012**, *112*, 1463–1535 and references therein.
- (11) Norel, L.; Rudolph, M.; Vanthuyne, N.; Williams, J. A. G.; Lescop, C.; Roussel, C.; Auchsbach, J.; Crassous, J.; Réau, R. *Angew. Chem., Int. Ed.* **2010**, *49*, 99–102.
- (12) (a) Nuckolls, C.; Katz, T. J. *J. Am. Chem. Soc.* **1998**, *120*, 9541–9544. (b) Katz, T. J. *Angew. Chem., Int. Ed.* **2000**, *39*, 1921–1923. (c) Nuckolls, C.; Katz, T. J.; Katz, G.; Collings, P. J.; Castellanos, L. J. *Am. Chem. Soc.* **1999**, *121*, 79–88. (d) Rahe, P.; Nimmrich, M.; Greuling, A.; Schütte, J.; Stará, I. G.; Rybáček, J.; Huerta-Angeles, G.; Starý, I.; Rohlfing, M.; Kühnle, A. *J. Phys. Chem. C* **2010**, *114*, 1547–1552. (e) Katz, T. J.; Sudhakar, A.; Teasley, M. F.; Gilbert, A. M.; Geiger, W. E.; Robben, M. P.; Wuensch, M.; Ward, M. D. *J. Am. Chem. Soc.* **1993**, *115*, 3182–3198.
- (13) (a) Reetz, M. T.; Beuttenmüller, E. W.; Goddard, R. *Tetrahedron Lett.* **1997**, *38*, 3211–3214. (b) Reetz, M. T.; Sostmann, S. J. *Organomet. Chem.* **2000**, *603*, 105–109. (c) Krausová, Z.; Šehnal, P.; Bondzic, B. P.; Chercheja, S.; Eilbracht, P.; Stará, I. G.; Šaman, D.; Starý, I. *Eur. J. Org. Chem.* **2011**, 3849–3857.
- (14) (a) Sato, I.; Yamashima, R.; Kadowaki, K.; Yamamoto, J.; Shibata, T.; Soai, K. *Angew. Chem., Int. Ed.* **2001**, *40*, 1096–1098. (b) Takenaka, N.; Sarangthem, R. S.; Captain, B. *Angew. Chem., Int. Ed.* **2008**, *47*, 9708–9710. (c) Chen, J.; Takenaka, N. *Chem.—Eur. J.* **2009**, *15*, 7268–7276. (d) Takenaka, N.; Chen, J.; Captain, B.; Sarangthem, R. S.; Chandrakumar, A. J. *Am. Chem. Soc.* **2010**, *132*, 4536–4537. (e) Crittall, M. R.; Rzepa, H. S.; Carbery, D. R. *Org. Lett.* **2011**, *13*, 1250–1253.
- (15) (a) *Introduction to Nonlinear Optical Effects in Molecules & Polymers*; Prasad, P. N., Williams, D. J., Eds.; John Wiley & Sons: New York, 1991.
- (16) (a) Champagne, B.; André, J. M.; Botek, E.; Licandro, E.; Maiorana, S.; Bossi, A.; Clays, K.; Persoons, A. *ChemPhysChem* **2004**, *5*, 1438–1442. (b) Kim, C.; Marks, T. J.; Facchetti, A.; Schiavo, M.; Bossi, A.; Maiorana, S.; Licandro, E.; Todescato, F.; Toffanin, S.; Muccini, M.; Graiff, C.; Tiripicchio, A. *Org. Electron.* **2009**, *10*, 1511–1520. (c) Bossi, A.; Licandro, E.; Maiorana, S.; Rigamonti, C.; Righetto, S.; Stephenson, G. R.; Spassova, M.; Botek, E.; Champagne, B. *J. Phys. Chem. C* **2008**, *112* (21), 7900–7907.
- (17) (a) Garcia, M. H.; Florindo, P.; Piedade, M. M.; Maiorana, S.; Licandro, E. *Polyhedron* **2009**, *28*, 621–629. (b) Ming, L. M.; Rose-Munch, F.; Rose, E.; Daran, J. C.; Bossi, A.; Licandro, E.; Mussini, P. R. *Organometallics* **2012**, *31*, 92–104.
- (18) Kawasaki, T.; Suzuki, K.; Licandro, E.; Bossi, A.; Maiorana, S.; Soai, K. *Tetrahedron: Asymmetry* **2006**, *17*, 2050–2053.

- (19) Monteforte, M.; Cauteruccio, S.; Maiorana, S.; Benincori, T.; Forni, A.; Raimondi, L.; Graiff, C.; Tiripicchio, A.; Stephenson, G. R.; Licandro, E. *Eur. J. Org. Chem.* **2011**, 5649–5658.
- (20) (a) Maiorana, S.; Papagni, A.; Licandro, E.; Annunziata, R.; Paravidino, P.; Perdicchia, D.; Giannini, C.; Bencini, M.; Clays, K.; Persoons, A. *Tetrahedron* **2003**, *59*, 6481–6488. (b) Rigamonti, C.; Ticozzelli, M. T.; Bossi, A.; Licandro, E.; Giannini, C.; Maiorana, S. *Heterocycles* **2008**, *76*, 1439–1470.
- (21) Usón, R.; Laguna, A.; Laguna, M. *Inorg. Synth* **1989**, *26*, 85–91.
- (22) SHELXTL 2008/1: Sheldrick, G. M. *Acta Crystallogr.* **2008**, *A64*, 112–122.
- (23) Parr, R. G.; Yang, W. *Density-Functional Theory of Atoms and Molecules*; Oxford Science Publication: New York, 1989.
- (24) Chai, J.-D.; Head-Gordon, M. J. *Chem. Phys.* **2008**, *128*, 084106.
- (25) Frisch, M. J.; et al. *Gaussian 09, Revision A.02*; Gaussian Inc.: Wallingford, CT, 2009.
- (26) (a) Casida, M. E. In *Recent Advances in Density Functional Methods, Part I*; Chong, D. P., Ed.; World Scientific: Singapore, 1995; pp 155–192. (b) Dreuw, A.; Head-Gordon, M. *Chem. Rev.* **2005**, *105*, 4009.
- (27) Plötner, J.; Tozer, D. J.; Dreuw, A. *J. Chem. Theory Comput.* **2010**, *6*, 2315–2324.
- (28) Harbach, P. H. P.; Dreuw, A. In *Modeling of Molecular Properties*; Comba, P., Ed.; Wiley: Weinheim, 2011; pp 29–47.
- (29) (a) Barone, V.; Cossi, M. *J. Phys. Chem. A* **1998**, *102*, 1995–2000. (b) Cossi, M.; Rega, N.; Scalmani, G.; Barone, V. *J. Comput. Chem.* **2003**, *24*, 669–681.
- (30) Van Overschelde, M.; Vervecken, E.; Modha, S. G.; Cogen, S.; Van der Eycken, E.; Van der Eycken, J. *Tetrahedron* **2009**, *65*, 6410–6415.
- (31) (a) Clot, O.; Akahori, Y.; Moorlag, C.; Leznoff, D. B.; Wolf, M. O.; Batchelor, R. J.; Patrick, B. O.; Ishii, M. *Inorg. Chem.* **2003**, *42*, 2704–2713. (b) Chen, B.-L.; Mok, K.-F.; Ng, S.-C. *J. Chem. Soc., Dalton Trans.* **1998**, 2861–2866.
- (32) Elfeninat, F.; Fredriksson, C.; Sacher, E.; Selmani, A. *J. Chem. Phys.* **1995**, *102*, 6153–6158.
- (33) Lachkar, A.; Selmani, A.; Sacher, E.; Leclerc, M.; Mokhliss, R. *Synth. Met.* **1994**, *66*, 209–215.
- (34) Bossi, A.; Maiorana, S.; Graiff, C.; Tiripicchio, A.; Licandro, E. *Eur. J. Org. Chem.* **2007**, 4499–4509.
- (35) Nakagawa, H.; Obata, A.; Yamada, K.-I.; Kawazura, H. *J. Chem. Soc., Perkin Trans. 2* **1985**, 1899–1903.
- (36) (a) Kutal, C. *Coord. Chem. Rev.* **1990**, *99*, 213–252. (b) Tiekinka, E. R.T.; Kang, J.-G. *Coord. Chem. Rev.* **2009**, *253*, 1627–1648. (c) Vogler, A.; Kunkely, H. *Coord. Chem. Rev.* **2002**, *230*, 243–251.
- (37) (a) Rodríguez, L.; Ferrer, M.; Crehuet, R.; Anglada, J.; Lima, J. C. *Inorg. Chem.* **2012**, *51*, 7636–7641. (b) Yam, V. W.-W.; Cheng, E. C.-C. *Chem. Soc. Rev.* **2008**, *37*, 1806–1813.
- (38) Bossi, A.; Falciola, L.; Graiff, C.; Maiorana, S.; Rigamonti, C.; Tiripicchio, A.; Licandro, E.; Mussini, P. R. *Electrochim. Acta* **2009**, *54*, 5083–5097.
- (39) Rausch, A. F.; Homeier, H. H. H.; Yersin, H. *Top. Organomet. Chem.* **2010**, *29*, 193–235.
- (40) Wang, D.; Cai, R.; Sharma, S.; Jirak, J.; Thummanapelli, S. K.; Akhmedov, N. G.; Zhang, H.; Liu, X.; Petersen, J. L.; Shi, X. *J. Am. Chem. Soc.* **2012**, *134*, 9012–9019.
- (41) (a) Hashmi, A. S. K.; Frost, T. M.; Bats, J. W. *J. Am. Chem. Soc.* **2000**, *122*, 11553–11554. (b) Hashmi, A. S. K.; Blanco, M. C.; Kurpejović, E.; Frey, W.; Bats, J. W. *Adv. Synth. Catal.* **2006**, *348*, 709–713. (c) Hashmi, A. S. K.; Rudolph, M.; Siehl, H.-U.; Tanaka, M.; Bats, J. W.; Frey, W. *Chem.—Eur. J.* **2008**, *14*, 3703–3708.
- (42) (a) Nieto-Oberhuber, C.; Muñoz, M. P.; Buñuel, E.; Nevado, C.; Cárdenas, D. J.; Echavarren, A. M. *Angew. Chem., Int. Ed.* **2004**, *43*, 2402–2406. (b) Jiménez-Núñez, E.; Echavarren, A. M. *Chem. Rev.* **2008**, *108*, 3326–3350. (c) Jiménez-Núñez, E.; Claverie, C. K.; Bour, C.; Cárdenas, D. J.; Echavarren, A. M. *Angew. Chem., Int. Ed.* **2008**, *47*, 7892–7895.
- (43) (a) Tarselli, M. A.; Gagné, M. R. *J. Org. Chem.* **2008**, *73*, 2439–2441. (b) Weber, D.; Tarselli, M. A.; Gagné, M. R. *Angew. Chem., Int. Ed.* **2009**, *48*, 5733–5736.
- (44) Hamilton, G. L.; Kang, E. J.; Mba, M.; Toste, F. D. *Science* **2007**, *317*, 496–499.